NOTICE

The quality of this microform is heavily dependent upon the quality of the original thesis submitted for microfilming. Every effort has been made to ensure the highest quality of reproduction possible.

If pages are missing, contact the university which granted the degree.

Some pages may have indistinct print especially if the original pages were typed with a poor typewriter ribbon or if the university sent us an inferior photocopy.

Previously copyrighted materials (journal articles, published tests, etc.) are not filmed.

Reproduction in full or in part of this microform is governed by the Canadian Copyright Act, R.S.C. 1970, c. C-30.

AVIS

La qualité de cette microforme dépend grandement de la qualité de la thèse soumise au microfilmage. Nous avons tout fait pour assurer une qualité supérieure de reproduction.

S'il manque des pages, veuillez communiquer avec l'université qui a conféré le grade.

La qualité d'impression de certaines pages peut laisser à désirer, surtout si les pages originales ont été dactylographiées à l'aide d'un ruban usé ou si l'université nous a fait parvenir une photocopie de qualité inférieure.

Les documents qui font déjà l'objet d'un droit d'auteur (articles de revue, tests publiés, etc.) ne sont pas microfilmés.

La reproduction, même partielle, de cette microforme est soumise à la Loi canadienne sur le droit d'auteur, SRC 1970, c. C-30.

Canada

THE UNIVERSITY OF ALBERTA

THE VERTICAL PROFILE OF SEA SPRAY CONCENTRATION OVER THE OCEAN SURFACE: A NUMERICAL SIMULATION

BY

YAHUI ZHUANG

A THESIS

SUBMITTED TO THE FACULTY OF GRADUATE STUDIES AND RESEARCH

IN PARTIAL FULFILMENT OF THE REQUIREMENTS FOR THE DEGREE OF

MASTER OF SCIENCE

IN

METEOROLOGY

DEPARTMENT OF GEOGRAPHY

EDMONTON, ALBERTA

FALL, 1987

ISBN 0-315-40939-8.

THE UNIVERSITY OF ALBERTA

RELEASE FORM

NAME OF AUTHOR: YAHUI ZHUANG

TITLE OF THESIS: THE VERTICAL PROFILE OF SEA SPRAY CONCENTRATION OVER THE OCEAN SURFACE: A NUMERICAL SIMULATION

DEGREE: MASTER OF SCIENCE

YEAR THIS DEGREE GRANTED: 1987

Yahui Zhuang

(Student's signature)

Chengdu Institute of Meteorology

Chengdu, Sichuan, China

(student's permanent address)

Date: July 8, 1987

THE UNIVERSITY OF ALBERTA

FACULTY OF GRADUATE STUDIES AND RESEARCH

The undersigned certify that they have read, and recommend to the Faculty of Graduate Studies and Research for acceptance, a thesis entitled THE VERTICAL PROFILE OF SEA SPRAY CONCENTRATION OVER THE OCEAN SURFACE ..... A NUMERICAL SIMULATION submitted by Yahui Zhuang in partial fulfilment of the requirements for the degree of Master of Science in Meteorology.

.....

.....

Co-Supervisor

.....

.....

Date: June 12, 1987

Abstract

The primary objective of this study is to calculate the vertical profile of the concentration of spray drops above the ocean surface, relating these to the controlling parameters (drop size and emission velocity, friction velocity, u_*, and surface roughness, z_0). The profiles are calculated using the trajectory simulation approach. By numerically simulating the stochastic turbulent trajectories of a very large number of ejected spray droplets (with a range of sizes and ejection velocities), the average liquid water content has been deduced as a function of height from the average residence time of the droplets in each of a set of horizontal layers above the ocean surface.

ACKNOWLEDGEMENTS

I would like to take this opportunity to express my sincere thanks to Dr. E.P. Lozowski and Dr. J.D. Wilson for their continuing encouragement and advice. Their clear and penetrating questions were much appreciated. I would also like to thank Dr. E.R. Reinelt and Dr. E.M. Gates for serving on my examining committee.

Thanks are extended to the Atmospheric Environment Service of Canada for funding that made possible my academic study and research. Finally, I am particularly grateful for assistance of Mr. A. Saulesleje of AES, who acted as the liaison for the contract.

TABLE OF CONTENTS

ABSTRACT IV

ACKNOWLEDGEMENTS V

TABLE OF CONTENTS VI

LIST OF FIGURES IX

NOMENCLATURE XI

1. INTRODUCTION 1

2. MODELLING THE TURBULENT TRAJECTORIES OF HEAVY PARTICLES 3

2.1 PHYSICAL CONSIDERATIONS FOR HEAVY-PARTICLE MOTION IN TURBULENT AIR 3

2.2 REVIEW OF EXISTING MODELS 6

2.3 FORMULATION OF A NEW MODEL 8

2.4 ASSESSMENT OF THE NEW MODEL 20

3. SIMULATION OF THE PROFILES OF LIQUID WATER CONTENT OVER THE OCEAN SURFACE 24

3.1 THE OCEANIC PRODUCTION RATES OF SEA SPRAY 24

3.2 SIZE DISTRIBUTION OF BUBBLES NEAR THE OCEAN SURFACE 24

3.3 SIZE DISTRIBUTION OF SEA SPRAY ABOVE THE OCEAN SURFACE 25

3.4 THE PROPOSED PRODUCTION RATES OF SEA SPRAY 26

3.5 EJECTION SPEEDS OF THE SEA SPRAY DROPLETS 30

3.6 MECHANISM FOR THE VERTICAL DISTRIBUTION OF SEA SPRAY 32

3.7 BOUNDARY LAYER PROPERTIES USED IN THE SIMULATION 34

3.8 EVAPORATION OF THE SPRAY DROPLETS IN THE MARINE BOUNDARY LAYER 38

3.9 THE RESULTS OF THE SIMULATION 39

4. DISCUSSION AND SUGGESTIONS FOR FURTHER RESEARCH 42

BIBLIOGRAPHY 44

APPENDIX A

A COMPUTER PROGRAM OF CALCULATING THE NUMBER DISTRIBUTION OF SEA-SPRAY 48

APPENDIX B

A COMPUTER PROGRAM FOR NUMERICAL SIMULATION OF SNYDER AND LUMLEY'S EXPERIMENT 50

LIST OF FIGURES

FIGURE PAGE

1. ILLUSTRATION OF THE VELOCITY CORRELATION OF THE SURROUNDING FLUID ELEMENTS 11

2. FLOW CHART OF THE TURBULENT TRAJECTORY MODEL 18

3. TURBULENT TRAJECTORY OF A HEAVY PARTICLE 19

4. THE WIND TUNNEL OF SNYDER AND LUMLEY'S EXPERIMENT 21

5. DISPERSION OF HEAVY PARTICLES IN A GRID-GENERATED TURBULENT FLOW 23

6. BUBBLE DENSITY FUNCTION NEAR THE OCEAN SURFACE UNDER ACTIVE BREAKING WAVE CONDITIONS 25

7. VOLUMETRIC FLUXES OF SEA SPRAY NEAR THE OCEAN SURFACE (AFTER WU et al.(1984)) 27

8. MASS FLUX OF SEA SPRAY AT THE OCEAN SURFACE 30

9. EJECTION SPEED OF JET DROPS 31

10. DROPLET TRAJECTORIES IN LAMINAR FLOW 32

11. SPRAY SIZE DISTRIBUTION FUNCTION (AFTER PREOBRAZHENSKII, 1971) 34

12. VARIATION OF THE PROFILES OF LIQUID-WATER CONTENT WITH ATMOSPHERIC STABILITY CONDITIONS 41

13. WIND DEPENDENCE OF THE PROFILES OF LIQUID-WATER CONTENT 41

14. PREDICTION OF THE SIZE DISTRIBUTION FUNCTION OF SEA SPRAY AT 10cm ABOVE THE OCEAN SURFACE 42

Nomenclature

Cd	drag coefficient
D	bubble diameter(μm)
d	particle diameter(μm)
$F(t-\tau)$	particle response function
$F_b(d_i)$	bubble size distribution function
$f_b(d_i)$	bubble size density function
F_b	buoyancy force acting on the bubble
Fd	drag force acting on the bubble
f_v	ventilation coefficient
g	gravitational acceleration
H	height of atmospheric boundary layer
ΔH_j	thickness of the jth atmospheric layer
k	molecular diffusivity of water vapor in the air
κ	Von Karman constant
L(f,g)	Eulerian length scales
$L_{m,o}$	Monin-Obukhov length
N_o	total number of bubble per unit volume
n	dynamic viscosity of water
P	atmospheric pressure
R	specific gas constant of air
R(Δt)	correlation coefficient of the driving fluid elements
Re	Reynolds number
Sc	Schmidt number
T(i,j)	the average residence time
T_L	Lagrangian integral time scale
Tm	temperature of air
U*	friction velocity
U_{ai}	velocity of fluid particle during the ith time step
U_{pi}	velocity of heavy particle during the ith time step
$\overline{U}(Z)$	mean flow velocity of the air
U'(t),W'(t)	velocity fluctuations of the air
V_d	rising speed of a bubble
W_o	ejection speed of a jet drop

X_{pi}, Z_{pi}	coordinates of the particle at the start of ith time step
z_o	roughness height
σ^2_p	velocity variance of heavy particles
$\sigma_{u,v,w}$	standard deviations of turbulent velocity
τ	time lag
τ_p	particle time constant
γ	surface tension of water
γ_{l+1}, η_{l+1}	independent standard normal random variables
$\Phi(z/L_{m,n})$	Non-dimensional profile for the transfer of momentum
α	the coefficient of Lagrangian temporal correlation and Eulerian spatial correlation
υ	kinematic viscosity of the air

Other symbols have their usual meaning.

1. Introduction

The study of the profile of liquid water content, in the air above the ocean surface, has great value not only in describing the processes that take place near the air-sea interface, but also in a number of applied problems such as ship icing or the construction of instruments and equipment for work under marine conditions. At the present time there is almost no theoretical literature on this subject known to the authors. There are only a few published experimental studies of the vertical variation of various types of sea spray.

The average liquid water content in the air above the ocean can be considered to be a result of the ejection of sea-spray droplets. During the disruption of the air-sea interface, caused by high wind velocities, an intense sea-spray is found in the atmospheric surface layer. Spray can be produced by the wind through various mechanisms: direct shearing of wave crests by the wind, aerodynamic suction at the crests of capillary waves, and the the bursting of air bubbles at the water surface. Bubble bursting has been considered by many authors to be the primary mechanism of spray production, since a large volume of air can be entrained by breaking waves (Wu,1979, 1984). In addition, sea-spray can be produced by impaction of waves on vessels or shore-based structures.

It is well known that increasing winds cause a proportional increase in the production of "whitecaps" at the sea surface. These "whitecaps" produce bubbles in the sea which, when they break at the surface, produce sea-spray over the surface. Therefore, it seems reasonable that some relation should exist between wind speed and the concentration of the sea spray.

Due to the turbulence over the ocean surface and the wind dependence of the production of the sea-spray, it is very difficult to determine the vertical flux of the sea-spray at different heights even if the initial flux at the surface is given. Rather than making an attempt to experimentally determine the flux of the sea spray, we decided to use a trajectory simulation method to indirectly deduce the average profile of sea spray concentration. If T(i,j) denotes the average residence time of the ith size particles in the jth layer(ΔH_j) of the atmosphere, and Q(i) denotes the mass ejection flux of ith particles from the ocean surface [kg m^{-2} s^{-1}], then $\Sigma Q(i)T(i,j)/\Delta H_j$ is the average sea spray concentration in the jth layer of the atmosphere.

The trajectory of a sea-spray droplet is a function of the turbulence and the physical properties of the particles. In the following sections a model of heavy particle trajectories in turbulent

flow is proposed, that incorporates the turbulent statistics and the properties of the heavy particles themselves (size, density). By using this model and the initial flux of the sea-spray, we have numerically calculated the liquid water content profiles of sea spray over the ocean surface.

2. Modelling the turbulent trajectories of heavy particles

2.1 Physical considerations for heavy-particle motion in turbulent air

The behaviour of discrete particles in a turbulent flow is a complex problem. If the particles are heavy or large compared with the scale of the turbulence, the main effect of the turbulence will be on the drag coefficient and the particles will follow the slower large-scale turbulent motion of the fluid. If the particles are light and small compared to the smallest scale of turbulence, they will respond to the entire spectrum of the air motion.

Theoretically little is known about the behaviour of particles with arbitrary densities and sizes. The following equation, derived most completely by Lumley(1957), relates the particles trajectories to their physical properties and the instantaneous fluid velocities:

$$\mathbf{X}_p(\mathbf{a}_o,t)=\mathbf{a}_o+\int_o^t \mathbf{U}_p(\tau)\,d\tau=\mathbf{a}_o+\int_o^t F(t-\tau)\mathbf{U}_s(\mathbf{X}_p(\mathbf{a}_o,\tau),\tau)\,d\tau \qquad (1)$$

where $\mathbf{a}_o$ is the initial particle position vector, $\mathbf{X}_p(\mathbf{a}_o,t)$ is the particle position, $\mathbf{U}_p(\tau)$ is the particle velocity, $F(t-\tau)$ is the particle response function which is determined by both turbulent fluctuations and the particle's inertial properties, and $\mathbf{U}_s(\mathbf{X}_p(\mathbf{a}_o,\tau),\tau)$ is the instantaneous velocity of a drifting fluid parcel.

In effect, equation (1) indicates that the particle motion depends not only on its initial position and its inertial parameters, but on a complete knowledge of the space-time field of the fluid motion. Usually such a complete description of the turbulent velocity field is not available and even if it were available, it would be determined only in a statistical sense. Conseqently, any solution of equation (1) must rest on physically based simplifying assumptions, and must be a statistical solution.

The paths of heavy particles in turbulent flow are complicated and different from those of the driving fluid elements for two reasons. First, because of their inertia, the heavy particles cannot follow exactly the high frequency fluctuations of the turbulent air. The greater the inertia the heavy particles have, the slower their response to the drifting fluid velocity. So there will always be some relative motion between the heavy particles and the surrounding fluid. Yudine (1959) first called this phenomenon the "INERTIAL EFFECT". Second, owing to the lack of coincidence between the velocity of heavy particles and that of the surrounding air, a heavy particle interacts consecutively with different air particles. In other words, the heavy particle will fall out of the eddy where it was at an earlier instant and enter a new eddy. Thus the velocity-history of the heavy particles will differ from those of marked fluid elements. Because of this, we might expect that the heavy particles lose their turbulence-velocity correlation more quickly than fluid elements, which change their turbulent velocities only owing to "eddy-decay". Yudine (1959) refered to this phenomenon as the "CROSSING TRAJECTORY EFFECT".

The " INERTIAL EFFECT" and "CROSSING TRAJECTORY EFF can be considered to be the crucial aspects of the heavy-particle motion in a turbulent flow. Of these, the first presents no great difficulty, but the second is hard to handle in a numerical model.

2.2 Review of existing models

Knowledge of the behaviour of discrete particles in a turbulent flow is of great interest to many branches of technology. In general, theoretical studies of heavy-particle motion fall into two categories: those which try to understand the behaviour of heavy-particle motion by formulating the Lagrangian autocorrelation function of the heavy particles, relating it to the turbulence statistics and the properties of the heavy particles (e.g. Yudine (1959),Csanady(1963), Meek and Jones(1973), Walklate(1987)), and those, based on the equation of motion of the heavy particles, which try to calculate both the particle velocity U_p and the surrounding fluid velocity U_a and then follow the heavy particle trajectory (e.g. Hunt and Nalpanis(1985), Faeth(1986)). The result of this latter method is a simple stochastic equation having an explicit solution which can be solved numerically.

In Meek and Jones' statistical analysis of heavy-particle motion in a turbulent fluid, they formulated an autocorrelation function of the heavy particle which can be deduced by assuming that the eddy is infinite. So in effect their model disregarded the "crossing trajectory effect". Walklate(1987) included the "crossing trajectory effect" but introduced an unknown coefficient C which varies with particle characteristics. In consequence these two models predicted that the ratio of particle velocity variance σ^2_p to

fluid velocity variance σ^2 is controlled only by τ_p/T_L (Meek and Jones's Equation(21), Walklate's Equation (14)), where τ_p is the particle time constant. Based on dimensional analysis and the evidence of Snyder and Lumley's experiment, Wilson et al.(1987) have suggested that the ratio σ^2_p/σ^2 is not a function of τ_p/T_L alone, but it depends on a number of other quantities also.

In Faeth's approach, the particles are assumed to interact with a succession of turbulent eddies as they move through the fluid. The fluid properties within a particular eddy are assumed to be uniform but change in a random fashion from eddy to eddy. A particle is assumed to interact with an eddy as long as the displacement of the particle with respect to the eddy does not exceed the characteristic eddy size, L_e and the time of the interaction does not exceed the characteristic eddy lifetime, T_e. With this model he obtained good agreement between the prediction results and Snyder and Lumley's experimental data. However, when Faeth's method is applied to the dispersion of very light particles, i.e, those approaching the density of air (in which case one can solve the problem using G.I. Taylor's analytical solution (Taylor,1921)) , it underestimates the rate of dispersion of the particles.

2.3 Formulation of a new model

The model to be described in this section is a random-walk method similar to Faeth's method. However it differs in the details of the treatment of the manner in which the particle is thought to interact with the surrounding fluid elements.

(1) Equation of motion

Consider Newton's second Law for a single rigid spherical particle in a turbulent flow (Soo,1967):

$$\begin{aligned}\frac{1}{6}\pi d^3\rho_p\left(\frac{dU_p}{dt}\right) = \quad & \frac{1}{6}\pi d^3\rho_p F(U_a - U_p) \\ & - \frac{1}{6}\pi d^3\frac{\partial p}{\partial r} \\ & + \frac{1}{12}\pi d^3\rho_a\frac{d(U_a - U_p)}{dt} \\ & + \frac{3}{2}d^2\sqrt{\pi\rho_a\mu}\int_{t_0}^{t}\frac{d(U_a - U_p)/d\tau}{\sqrt{t-\tau}}\,d\tau \\ & + \frac{1}{6}\pi d^3\rho_p g\end{aligned} \qquad (2)$$

The meaning of the various terms is as follows:

The term on the left-hand side is the product of the particle mass and acceleration. The first term on the right-hand side is the drag force. The second term is due to the pressure gradient in the fluid

surrounding the particle. The third term is the force required to accelerate the virtual "added" mass of the particle relative to the ambient fluid. The fourth term is the so-called "Basset" term, which takes into account the cumulative effect of the deviation in the flow around the particle from steady state. The last term is the gravitational force. As long as the ratio of particle density to the fluid density is very large (>10^3), the second, third and fourth terms on the right-hand side can be ignored with little error. Thus the simplified Equation of motion is approximately given by:

$$\frac{dU_p}{dt} = F(U_a - U_p) - g \qquad (2')$$

where $F = .75\frac{C_d \rho_a}{d \rho_d}|U_a - U_p|$

C_d is the drag coefficient which is given(Schlichting, 1960) by

$$C_d = \frac{24}{Re}(1 + 3x\frac{Re}{16}) \qquad Re<5$$

and the Reynolds number Re is given by

$$Re = d \times \frac{|U_a - U_p|}{\nu}$$

For a given U_a and the initial U_p, Equation (2') can be integrated numerically for future values of U_p. Since U_a is the velocity of the surrounding fluid encountered by the particle and the surrounding fluid does not remain the same all the time but changes

irregularly, Equation (2') is a nonlinear stochastic equation. The core of the problem now lies in the determination of the time series of fluid velocity U_a[$U_a = U(Z) + U'_a$] which is neither an Eulerian nor a fluid Lagrangian sequence. Usually there exists some correlation between the values of the velocities of the surrounding fluid at any two times (see Fig.1.) such that

$$\frac{\overline{U'_a(t_1) U'_a(t_2)}}{\overline{U'^2_a}} = R(t_2 - t_1) \qquad (3)$$

where $\overline{U'^2_a}$ = mean square fluid velocity summed over all fluid particles.

If the correlation coefficient $R(t_2-t_1)$ were known, we might be able to solve the velocity sequence U_a using the method of Markov chain simulation (Wilson, el at 1981). In general, the correlation will vary from approximately the Lagrangian fluid correlation for extremely light and small particles to the Eulerian spatial correlation for very heavy and large particles. Unfortunately, except for the two extreme cases, this correlation is unknown. However these two correlations could provide a guide for extremes in particle behaviour.

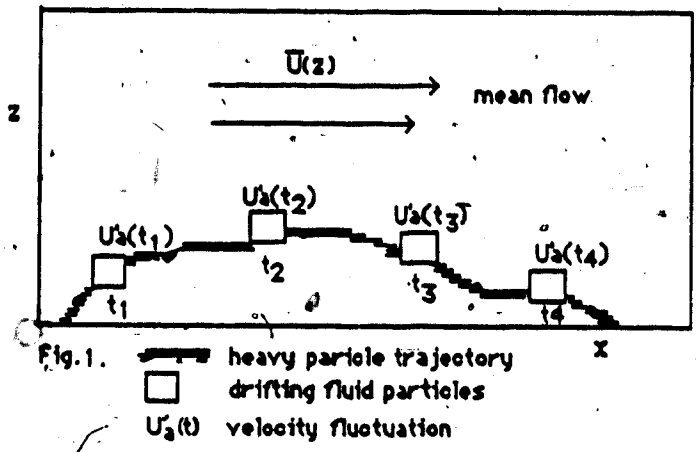

Fig.1.

(2) Turbulent trajectory model

In recent years, random-walk theory has been used intensively to model atmospheric diffusion (i.e. Reid,1979; Wilson et al, 1981; Ley and Thomson,1983). In these situations it has been assumed that the particles behave as marked particles of air (i.e. that the turbulence characteristics of tracer particles are the same as those of atmosphere). So one can predict the motion of tracer particles as long as the turbulence statistics, and the mean flow are known. As for the motion of heavy particles, their behaviour is much more complex than that of the air itself. In order to model the motion of heavy particles, one needs more information about the properties of the turbulence and the particles. In this model it is found that the Eulerian length scales are needed, in addition to the turbulence properties used in the model of the motion of tracer particles.

The model is based on the following assumptions:

——The statistics of the space-time field of the turbulence are known.

——The velocity of the fluid particles in the neighbourhood of the heavy particle can be determined from the fluid Lagrangian velocity correlation and the Eulerian spatial velocity correlation (as apparently first suggested by Peskin see Hinze(1975), p.470).

(a) Fluid Turbulent Velocity

The turbulent flow field is described by a sequence of eddies the stochastic properties of which are found by making a random selection from a Gaussian probability density function of the velocity.

The spatial velocity correlation between different fluid elements at a fixed time can be described by the Eulerian length scale L which is to a certain extent a measure of the longest correlation distance between the simultaneous velocities at two points of the flow field (Hinze(1975), p.43). The Eulerian spatial correlation coefficient can be expressed as:

$$\frac{\overline{u_s'(r_1,t)\,u_s'(r_2,t)}}{\overline{u_s'^2}} = e^{-\frac{|r_2-r_1|}{L}} \qquad (4)$$

The correlation of the velocities of a particular fluid particle at two different times (t_1, t_2) is described by the Lagrangian integral time scale T_L which is usually considered as a measure of the longest time during which, on the average, a particle persists in a motion in a given direction(Hinze(1975), p.53). The Lagrangian autocorrelation coefficient can be expressed as:

$$\frac{\overline{U_a(t_1)U_a(t_2)}}{\overline{U_a^2}} = e^{-\frac{t_2 - t_1}{T_L}} \qquad (5)$$

The overbar denotes an ensemble average over different "realizations" of the flow. It should be noted that using the above exponential functions to represent the Eulerian spatial correlation and Lagrangian time correlation is only an approximation. The exact forms of these correlations are unknown.

(b) Droplet Velocity

The coordinates of the heavy particle at the start of the ith time step are denoted by X_{pi}, Z_{pi}, and the velocity components during the time step by U_{pi}, W_{pi}. The velocity components of the driving fluid element are U_{ai}, W_{ai}.

The governing equations and the equations relating the values of U_{ai}, W_{ai}, X_{pi}, Z_{pi}, U_{pi}, W_{pi} at successive time steps are:

$$\frac{dU_{pi}}{dt} = F(U_{ai} - U_{pi}) \qquad (2a)$$

$$\frac{dW_{pi}}{dt} = F(W_{ai} - W_{pi}) - g \qquad (2b)$$

$$X_{pi+1} = X_{pi} + U_{pi}\Delta t \qquad (6a)$$

$$Z_{pi+1} = Z_{pi} + W_{pi}\Delta t \qquad (6b)$$

$$U'_{ai+1} = U'_{ai}\alpha + \lambda_{i+1} \qquad (6c)$$

$$U_{ai+1} = U'_{ai+1} + U(z) \qquad (6d)$$

$$W_{ai+1} = W_{ai}\alpha + \mu_{i+1} \qquad (6e)$$

where $\alpha = e^{-\left(\frac{\Delta t}{T_L} + \frac{\Delta r}{L}\right)}$ is the coefficient of Lagrangian temporal correlation and Eulerian spatial correlation. Δt is the time

interval which is much smaller than T_L, Δr is the distance between the position of the fluid element the particle interacted with at the previous time step and the position of the fluid element with which the particle is now interacting. λ_{i+1} and μ_{i+1} are random variables whose properties are chosen in order to ensure that the fluid elements move in accordance with the known turbulence statistics, i.e ,λ_{i+1} and μ_{i+1} must be chosen to satisfy:

$$\lambda_{i+1} = (1-\alpha^2)^{\frac{1}{2}}\,\sigma_u\,\gamma_{i+1}$$

$$\mu_{i+1} = (1-\alpha^2)^{\frac{1}{2}}\,\sigma_w\,\eta_{i+1} \qquad (7)$$

where γ_{i+1} and η_{i+1} are the independent standard normal random variables, σ_u and σ_w are the standard deviations of turbulent velocity in the horizontal and vertical directions respectively*.

* These two random variables are selected to give the sequence (U_{ai}, W_{ai}) the correct variances (Legg et al,1982). Theoretically α must be a constant in this formula, but simulation shows that with a variable α one still obtains correct variances.

Referring to Figure 2, the relationship assumed between the "driving" fluid velocities at consecutive times is as follows: the "initial" fluid element shown at position A at time T1 moves during the timestep to a new position B at time T2 where its velocity $U^*_a(T2)$ is assumed to be composed of a fraction of its velocity at time T1 (the fraction being governed by the Lagrangian fluid velocity correlation for time lag T2-T1) and a random change. However the fluid velocity we require at time T2, $U_a(T2)$, is at the new heavy particle location C which does not coincide with the present position B of the "initial" fluid element. The new "driving" velocity is taken to be the sum of a fraction of the present fluid velocity $U^*_a(T2)$ at B (the fraction being governed by the Eulerian spatial velocity correlation for separation r(B)-r(C)) and a random change.

This model includes the "inertial effect" naturally. Equations (6c), (6d), and (6e) account for both the Eulerian spatial decorrelation and the Lagrangian temporal decorrelation described above. Furthermore, a heavy particle is assumed to interact with a particular eddy as long as the displacement of the particle with respect to the eddy does not exceed the average eddy size. When the displacement between the initial fluid parcel and the heavy particle, R, exceeds the average eddy size, the particle is assumed to have moved out of the old eddy and to have entered a new eddy. We then

create a new eddy whose properties are found by making a random selection from the P.D.F of velocity and continue the calculation*. The average eddy size is chosen to be the Eulerian length scale.

Under the above arguments, the motion of a heavy particle in a turbulent flow can be simulated using Equations (2') and (6). Fig.3 shows a schematic flow chart of the heavy-particle trajectory model.

*In fact, equations (6c) and (6e) should be sufficient to account for the "crossing trajectory effect" (see Peskin 1962, Walklate 1987), but we found this resetting of the chain to be necessary.

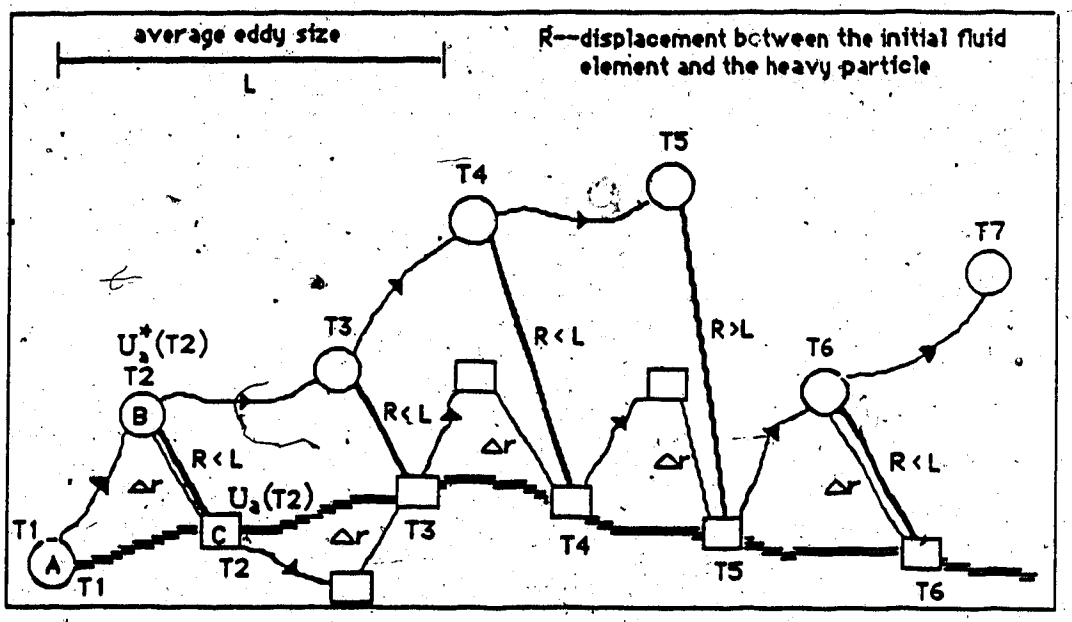

Fig.2. Turbulent trajectory of a heavy particle

Heavy particle trajectory

Fluid element trajectory

Initial fluid element

Driving fluid element

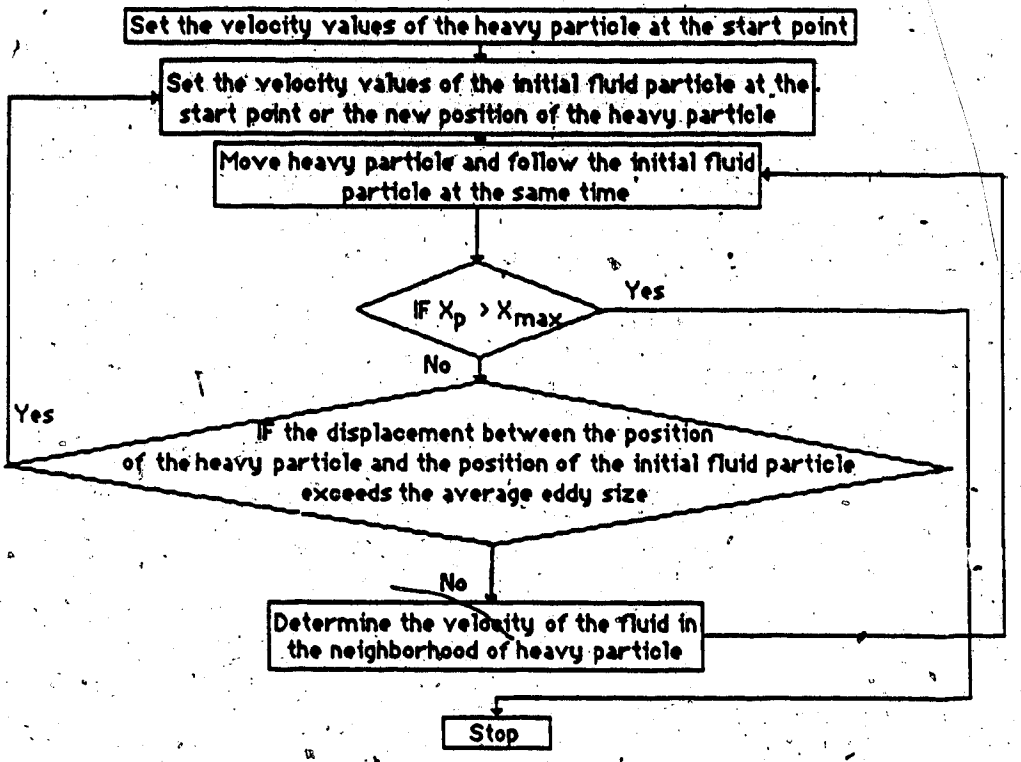

Fig.3. Flow chart of heavy particle trajectory model

2.4 Assesment of the new model

There is little literature on the experimental measurement of heavy-particle motion in turbulent flow. To assess models of heavy-particle motion in turbulent flow most people(Faeth(1986), Meek and Jones(1973), Walklate(1987)) have used Snyder and Lumley's experimental data. The measurements of Snyder and Lumley (1971) involved dispersion of various types of individual particles which were injected into decaying turbulence downstream of a wind tunnel grid (see Fig.4.). Comprehensive turbulence data are given, in addition to particle velocity and dispersion data.

In order to simulate the heavy-particle motion in decaying turbulence, we have to account for the streamwise variation of the fluid velocity statistics. The simulation of these experiments with this model was undertaken with the following air turbulence and mean flow data for a vertically upward flow in the Z direction (see table1.).

Table 1.

Mean flow	$U=0$	
	$V=0$	
	$W=6.55$	m/s
Variances of turbulent velocity	$\sigma_u^2 = 6.55^2/(39.4(39.3Z+8))$	$(m/s)^2$
	$\sigma_v^2 = \sigma_u^2$	$(m/s)^2$
	$\sigma_w^2 = 6.55^2/(42.4(39.3Z+4))$	$(m/s)^2$

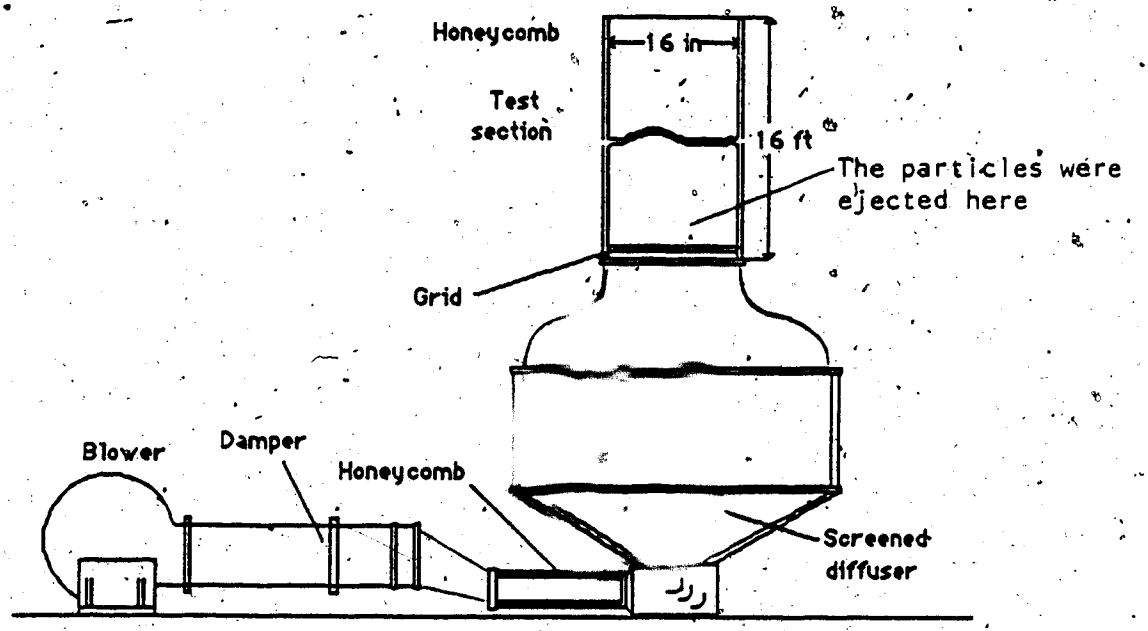

Fig.4. The wind tunnel of Snyder and Lumley's experiment

Based on the experimental data (Snyder and Lumley (1971), table2) and Snyder and Lumley's analysis of the decay of the turbulent flow we derived the Eulerian integral length scales for both the streamwise and the cross-stream directions:

$$L_f = .0034(39.3Z+32)^{0.5}$$
$$L_g = .4L_f \qquad (8)$$

The Lagrangian integral time scale T_L is assumed to be L_g/σ_u in accordance with Snyder and Lumley's conclusion (most previous models took T_L as a constant, but according to Snyder and Lumley's suggestion, T_L should vary linearly with (39.3Z+32)). The average eddy size is chosen to be Lg. One thousand particle trajectories were calculated for each of the different particle sizes in order to get a statistically stable solution. The results of the predictions and the corresponding measurements are illustrated in Fig.5. The simulations are in reasonably good agreement with the measurements for both light particles (hollow glass beads) and heavy particles (copper beads), although the agreement for corn pollen is not quite as good.

In the following sections, this model is applied to the problem of calculating sea-spray trajectories. Combined with the boundary layer condition, the profile of average liquid water content over the ocean surface has been deduced.

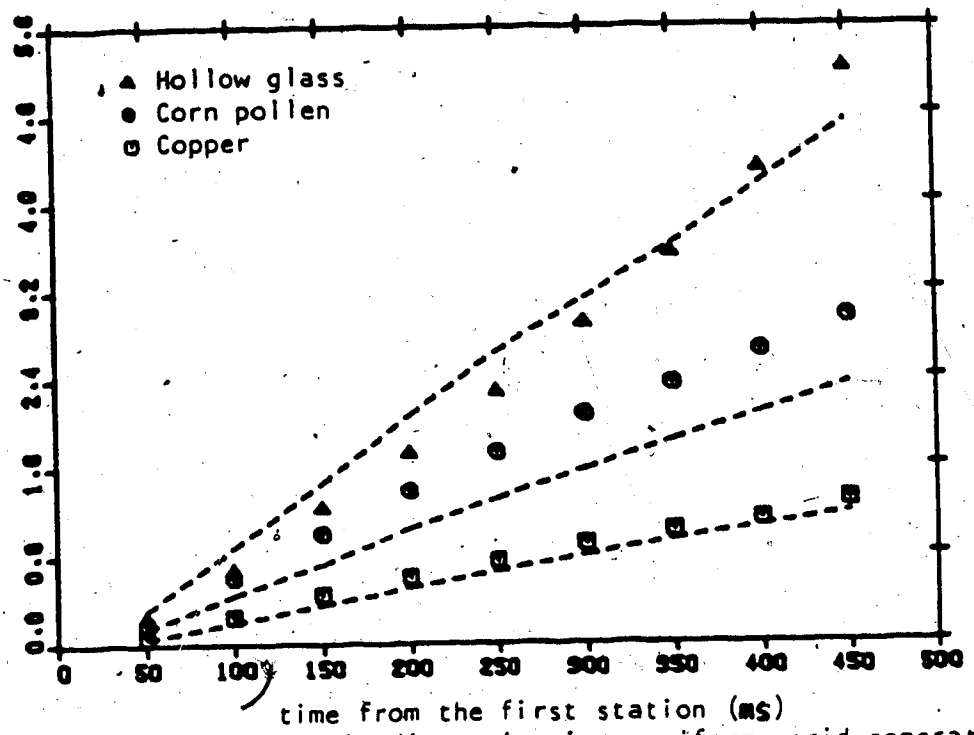

Fig.5 Heavy particle dispersion in a uniform, grid-generated turbulent flow

(▲ ● ⊎) Snyder and Lumley's experiment

---------- Prediction

3. Simulation of the profiles of liquid water content over the ocean surface

3.1 The oceanic production rates of sea sprays

The production rate of sea-spray depends on a number of factors, namely, those that determine the spectrum of bubbles that break at the sea surface (the distribution of bubbles, the relationship between the bubbles and the sea-spray, etc). Because there is very little literature on this subject, we will make some quantitative assumptions in order to deduce the emission fluxes.

3.2 Distributions of bubbles near the ocean surface

Recently Kerman (1986) proposed a model for the bubble size density function (f_b) near the ocean surface under active breaking wave conditions:

$$f_b(d_i) = 3\frac{d_i^2}{\langle d\rangle^3} e^{-\frac{d_i^3}{\langle d\rangle^3}} \qquad (9)$$

Where <d> is the expectation or mean value of the bubble diameter. Fig.6 shows the theoretical bubble density function calculated from (9). The bubble size distribution function is then expressed as:

$$F_b(d_i) = 3N_o^* \frac{d_i^2}{\langle d\rangle^3} e^{-\frac{d_i^3}{\langle d\rangle^3}} \Delta d_i \qquad (10)$$

where N_o^* is the total number of bubbles per unit volume in a layer of thickness comparable to the largest cavities near the interface. It is given by:

$$N_o^* = \xi \times 5.233 \times U_*^3 \qquad (11)$$

The similarity coefficient ξ was estimated to be of the order of unity.

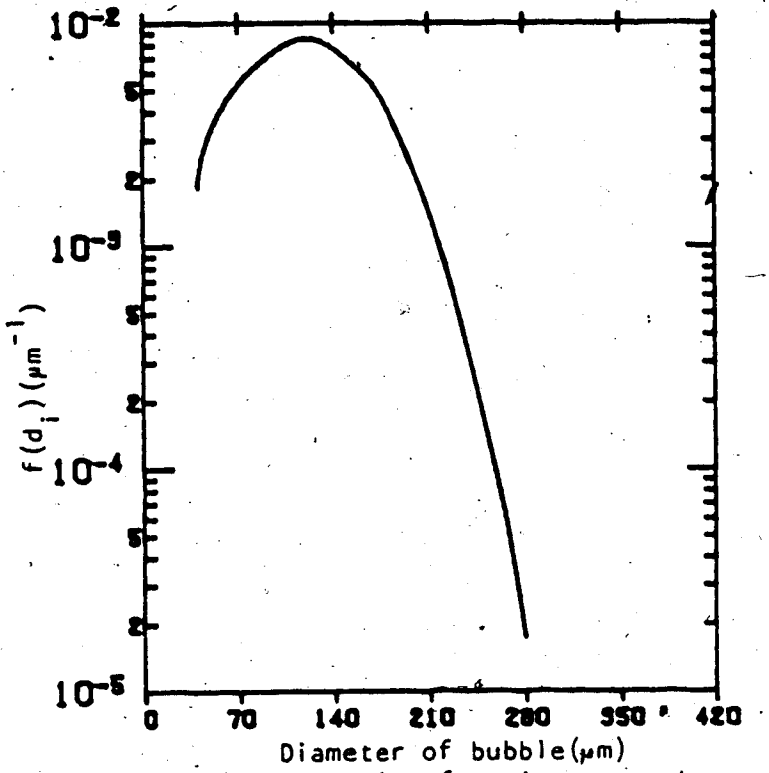

Fig.6 Bubble size density function near the ocean surface under active breaking wave condition as given by (9)

3.3 Distribution of sea-spray above the ocean surface.

If droplet numbers are proportional to the number of the

bubbles, we might expect that the spray droplet distribution function at the surface would have a similar form to that of the bubble distribution function although at higher levels the droplet distribution function will be greatly influenced by turbulent mixing and gravitational settling. In fact, when assuming that the liquid is dispersed into droplets in a completely random way with respect to the volumes of the droplets, Angelidou et al. (1979) derived the following size density function for droplets:

$$f_D(D_1) = 3\left(\frac{\Gamma(\frac{3}{4})}{\langle D\rangle}\right)^3 D_1^2 e^{-\left(\frac{\Gamma(\frac{3}{4})D_1}{\langle D\rangle}\right)^3} \qquad (12)$$

Equation (12) is similar to equation (9). Wu(1981) has noted the similarity in the droplet size distribution of Preobrazhenskii (1973) with the bubble size distribution of Kolovayer(1976).

3.4 The proposed production rate of sea spray

Wu(1979) observed that the production rate of sea-spray varies in a power law form with the wind friction velocity U_*. Later, Wu et al.(1984) carried out an experiment to measure the production rate of sea spray. The measured spectrum of volumetric fluxes of sea spray near the surface is shown in Fig.7.

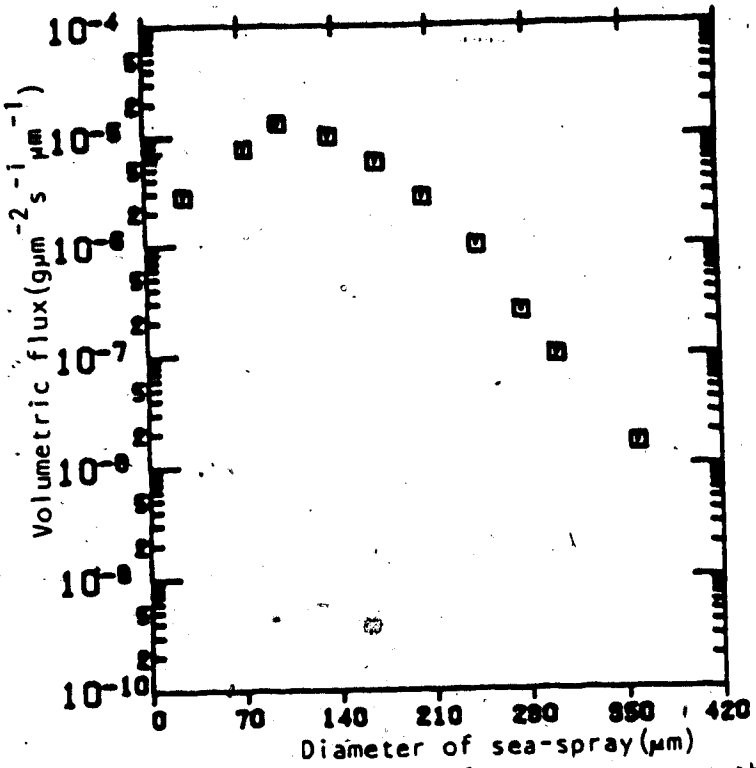

Fig.7 Volumetric fluxes of sea-spray near the ocean surface (After Wu et al.,1984)

Comparing Fig.6. and Fig.7., it seems reasonable to assume some relationship between the bubble size distribution function and the ejection flux of the sea spray. For simplicity we assume that the bubbles are all distributed uniformly to the same depth, all bubbles reaching the surface burst and one bubble produces one droplet. Then the ejection rates of the sea spray can be computed from the concentration of the bubbles $F_b(d)$ (these bubbles produce the jet

drops ejected at the ocean surface) multiplied by the rising rate of the bubbles, V_d,

$$Q(d,V_d)=F_b(d)*V_d \qquad (13)$$

where the rising rates of bubbles V_d can be calculated in the following manner. There are two forces (drag force and buoyancy force) acting on a bubble in the water. The expression for the drag force is:

$$Fd=3*\pi*n*V_d*d*(C_d*Re/24) \qquad (14)$$

where n is the dynamic viscosity of the water; d is the bubble diameter; Re is the Reynolds number.

The buoyancy force on the bubble is:

$$F_b=\frac{1}{6}\pi d^3 g(\rho_w-\rho_a) \qquad (15)$$

where g is the gravitational acceleration and ρ_w and ρ_a are the densities of sea water and air, respectively.

Assuming a steady state, the drag force equals the buoyancy force; that is:

$$3\pi n d V_d \left(\frac{C_d Re}{24}\right) = \frac{1}{6}\pi d^3 g(\rho_w - \rho_a) \qquad (16)$$

Moore (1959) examined the motion of spherical air bubble and gave $C_d = 31/Re$. Subsituting C_d into Equation (16), the rising rate of bubbles is:

$$V_d = 4.3\times 10^{-2}\,\frac{d^2(\rho_w - \rho_a)g}{n} \qquad (17)$$

Mason (1954) reported that the size of the jet droplet is directly ralated to the size of the bubbles and is about 15% of the size of the bubbles. Consequently the rising rate of the bubble can be expressed in terms of the diameter of the spray droplet as:

$$Vd = 1.91\,\frac{D^2(\rho_w - \rho_a)g}{n} \qquad (18)$$

Fig.8. shows a comparison of the ejection mass flux calculated from $Q(d_i, V_d)$*mass(d_i) with the experimental data of Wu et al.(1984).

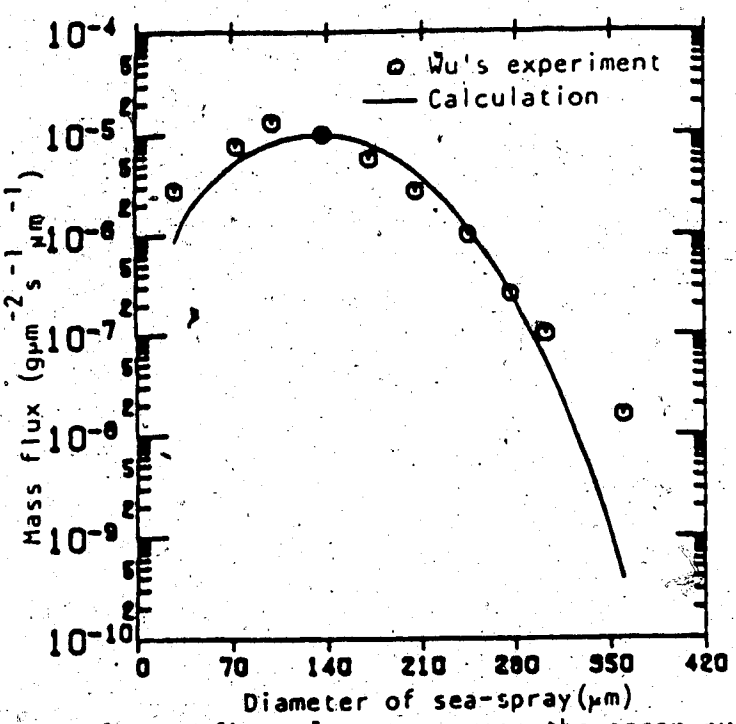

Fig.8 Mass flux of sea-spray at the ocean surface

The agreement is fairly good. This may imply that the Equation (13) is a reasonable approximation for the ejection rate of the sea spray.

3.5 The ejection speed of the sea-spray droplets

Newitt,D.M. et al (1954) studied the breaking of bubbles and worked out an expression for the speed of the rising jet by considering the relationship between the forces acting on the crater:

$$W_o = \frac{3}{2} \frac{(P + \frac{4\gamma}{D})t}{\rho_w D} \qquad (19)$$

Where W_o is the ejection speed of jet drop; P is the atmospheric pressure; γ is the surface tension; d is the bubble diameter; and t is the acting time of the vertical impulse force, which is assumed to be 30ms. It was claimed by Newitt that the value of W_o calculated from formula (19) and the observed value of Wo are in fair agreement. Since D=.15d, the ejection speed of the jet droplets can be written approximately as:

$$W_o = 0.225(\frac{P + \frac{0.6\gamma}{D}}{\rho_w D})t \qquad (20)$$

Fig.9 shows the variation of ejection speed with the spray diameter as calculated from (20).

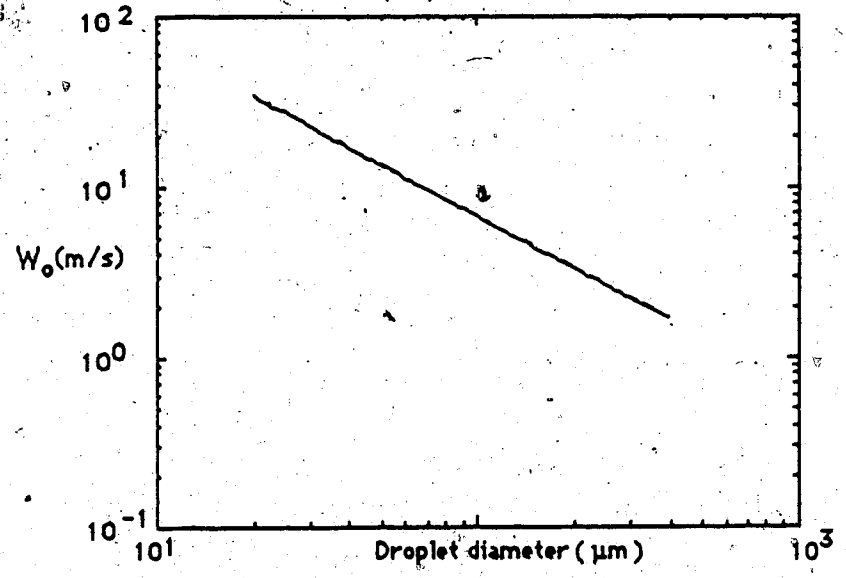

Fig.9. Election speed of jet drop

3.6 Mechanism of the vertical distribution of sea spray

Measurements (Preobrazhenskii,1971) have shown that sea spray can be observed at a height of more than 10 meters above the ocean surface in the atmospheric boundary layer. But from both calculation (see Fig.10) and the experimental data (Blanchard and Woodcock,1957) of sea spray trajectories in laminar flow, It is found that the maximum ejection height of the droplets is less than 20 cm due to the drag and gravitational forces acting on them.

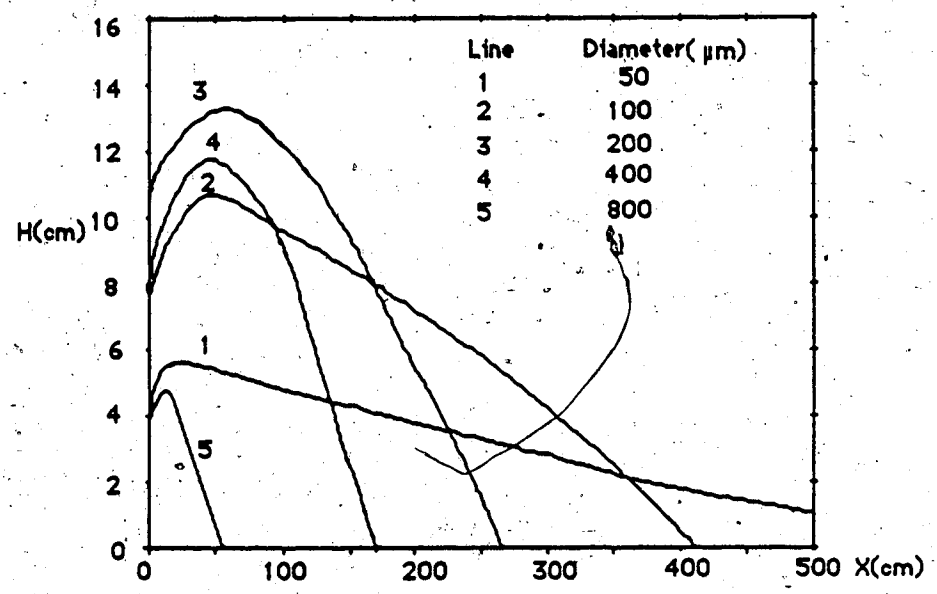

Fig.10 Droplet trajectories in a laminar flow

Obviously the mechanism of the motion of sea spray in the atmospheric boundary layer must be different from that in laminar flow.

Once the sea spray droplets are ejected into the turbulent air, they are influenced by gravity which tends to carry them back to the sea. On the other hand, due to the turbulent velocity, the drag force tends to distribute them in all directions. In the meantime, evaporation tends to reduce gravitational settling by decreasing particle mass. The large droplets are not readily carried above the near surface air layer by atmospheric turbulence, and they cannot stay in the air for a sufficient period of time for them to evaporate significantly. Much smaller droplets are light enough to be readily mixed upward by atmospheric turbulence, and if the air is unsaturated with respect to water vapor, they will undergo appreciable evaporation which will further favor their upward transport. Because of the difference between these motions of small and big droplets, we expect that the particle size distribution function must change with height, i.e, there will be more big drops in the lower layer than in the higher layer, and the small drop concentration will vary slowly with height, as shown in Fig.11.

The final distribution of sea-spray particles over the ocean surface will largely depend on (1) the rates of production of sea-spray droplets, (2) the turbulence in the air, and (3) the rate of evaporation.

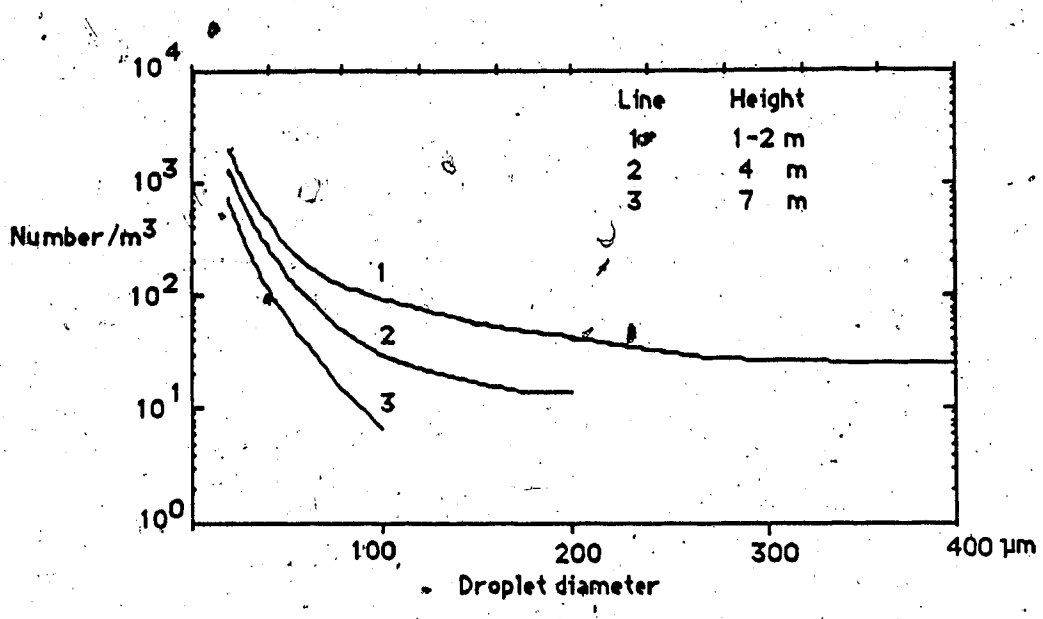

Fig.11 Spray size distribution (after Preobrazhenskii,1971)

3.7 Boundary layer properties used in the simulation.

The boundary layer properties must be specified in addition to the initial flux of the sea-spray. The simulation of sea-spray concentration is determined greatly by the boundary layer turbulence as has been mentioned in 3.6.

A The marine boundary layer

In general, according to the Monin-Obukhov similarity theory (Monin and Obukhov,1954), the spectra and cospectra of turbulence in the atmospheric surface layer are considered to have universal forms described by parameters such as the friction velocity and the stability parameter. The atmospheric surface layer has been

extensively studied over land, but fewer studies have been made at sea. At least two differences exist between the marine and land surface layers. Firstly, the latent heat flux loss from the ocean dominates the total heat flux loss and the latent heat flux can also contribute to buoyancy effects. Secondly, there is some evidence suggesting that the velocity statistics are not unaffected by the presence of a moving wavy surface as a lower boundary (Takeda, 1981). In spite of the differences of physical properties between the sea surface and land, measurements (Schmitt,K.F.,1979) have demonstrated the validity of Monin-Obukhov similarity theory over the sea.

B Wind profile

Dimensional analysis, following the Monin-Obukhov similarity theory, leads to the following relationship in the atmospheric surface layer:

$$\frac{d\bar{U}(Z)}{dz} = \frac{U*}{\kappa Z}\Phi\left(\frac{Z}{L_{m,o}}\right) \qquad (21)$$

where U(z) is the average wind, and $\Phi(z/L_{m,o})$ is a universal function (Dyer,1974) given by:

$$\Phi\left(\frac{Z}{L_{m,o}}\right)=\begin{cases}1+5z/L_{m,o} & L_{m,o}>0\\ (1-16Z/L_{m,o})^{-\frac{1}{4}} & L_{m,o}<0\end{cases} \quad (22)$$

The Monin-Obukhov length $L_{m,o}$ is given by

$$L_{m,o}=-\frac{\rho_a C_p T_m U_*^3}{\kappa g H} \quad (23)$$

C Turbulent fluctuations and statistics

The analysis of turbulent characteristics in boundary layer from the experiments by Caughey et al. (1979) and Panofsky et al. (1977) can be represented as follows:

(1) Turbulent fluctuations

$$\sigma_w=\begin{cases}1.3U_*(1-Z/L_{m,o}) & L_{m,o}>0\\ 1.3U_* & L_{m,o}=0\\ 1.3U_*(1+3|Z/L_{m,o}|)^{\frac{1}{3}} & L_{m,o}<0\end{cases} \quad (24)$$

$$\sigma_u=\begin{cases}2.3U_*(1-Z/H) & L_{m,o}>0\\ 2.3U_* & L_{m,o}=0\\ U_*(12+.5|H/L_{m,o}|)^{\frac{1}{3}} & L_{m,o}<0\end{cases} \quad (25)$$

(2) Length and time scales

(a) Lagrangian integral time scale T_L

$$T_L = \begin{cases} 0.4ZU*/(1+5\,Z/L_{m,o})\sigma_w^2 & L_{m,o} > 0 \\ 0.26Z/U* & L_{m,o} = 0 \\ 0.4ZU*(1+16|Z/L_{m,o}|)^{\frac{1}{2}}/\sigma_w^2 & L_{m,o} < 0 \end{cases} \quad (26)$$

(b) Eulerian Length scale

$$L = T_L * \sigma_w \quad (27)$$

D Boundary Layer Height

The expression for turbulent fluctuations depends on the boundary layer height which is a complicated and unpredictable function of time. We have chosen to impose characteristic values.

$$H = \begin{cases} 200\ m & \text{stable} \\ 1000\ m & \text{unstable} \end{cases} \quad (28)$$

3.8 Evaporation of the spray droplets in the marine boundary layer

The evaporation rate of small water droplets in the air has been studied by Beard and Pruppacher (1971). The rate of evaporation can be written as:

$$\frac{dM}{dt} = -f_V \frac{2\pi DK}{1-(e_D + e_a)/2P} \frac{e_D - e_a}{RT_m} \tag{29}$$

where f_V is the ventilation coefficient for mass transfer, given by

$$f_V = \begin{cases} 1+0.108N^2 & N < 1.4 \\ 0.78+0.308N & N > 1.4 \end{cases} \qquad (N = Sc^{\frac{1}{3}} Re^{\frac{1}{2}}) \tag{30}$$

M is the mass of the droplet; k is the diffusivity of water vapor in the air; R is the specific gas constant for water vapor; e_d and e_a are the vapor pressures at the surface of the droplets and in the air respectively, and Sc is the Schmidt number. Wu(1979) pointed out that the above empirical formula was derived for laminar flow and would therefore underestimate the evaporation effect. Consequently, we can only estimate the lower bound of the evaporation rate since no study has been reported on the evaporation of small water drops in turbulent flow. In the following simulation, the relative humidity and the temperature are chosen to be 80% and 5°C, respectively.

3.9 The results of the simulation

Simulation of the vertical liquid water content has been computed with the equations: (2), (6), (7), (13), (18), (20), and the boundary layer conditions given in 3.7. Ten categories (20,····· 200μm) of drop size have been assumed. Theoretically each of these droplets must be followed until either it evaporates completely or it falls down to the sea surface. In practice, however, it is impossible to track the very small particles (< 10μm) due to limited computing time. The simulation of a particle trajectory is ended when one of the following three criteria is satisfied: (1) the particle falls down at the sea surface, (2) the particle is evaporated to a size less than 10μm, (3) the particle has moved horizontally over 100 metres. Fig.12. shows the variation of the profiles of liquid-water content with atmospheric stability*. The simulation predicts that the more unstable the air is, the higher the spray will be found, as expected. Unfortunately there are no corresponding measurements to compare with. Fig.13. shows the wind dependence of the profiles. The simulation is quite sensitive to the friction velocity. When the friction velocity increases from 0.2m/s to 0.5m/s, the liquid water

---

The curves in fig.12 and fig.13 are not smooth, which may be due to the limited number of drop size categories assumed.

content increases rapidly. This is because the friction velocity characterizes the wind and the wave structure, and consequently the spray production. The size distribution function of the sea spray at 10cm above the ocean surface has been simulated as shown in Fig.14. This distribution function is quite similar to the size distribution function of bubbles found by Wu(1981). Such a result may indicate that the production efficiency of the sea spray droplets from bubbles is approximately constant in the drop size range of 20-400μm.

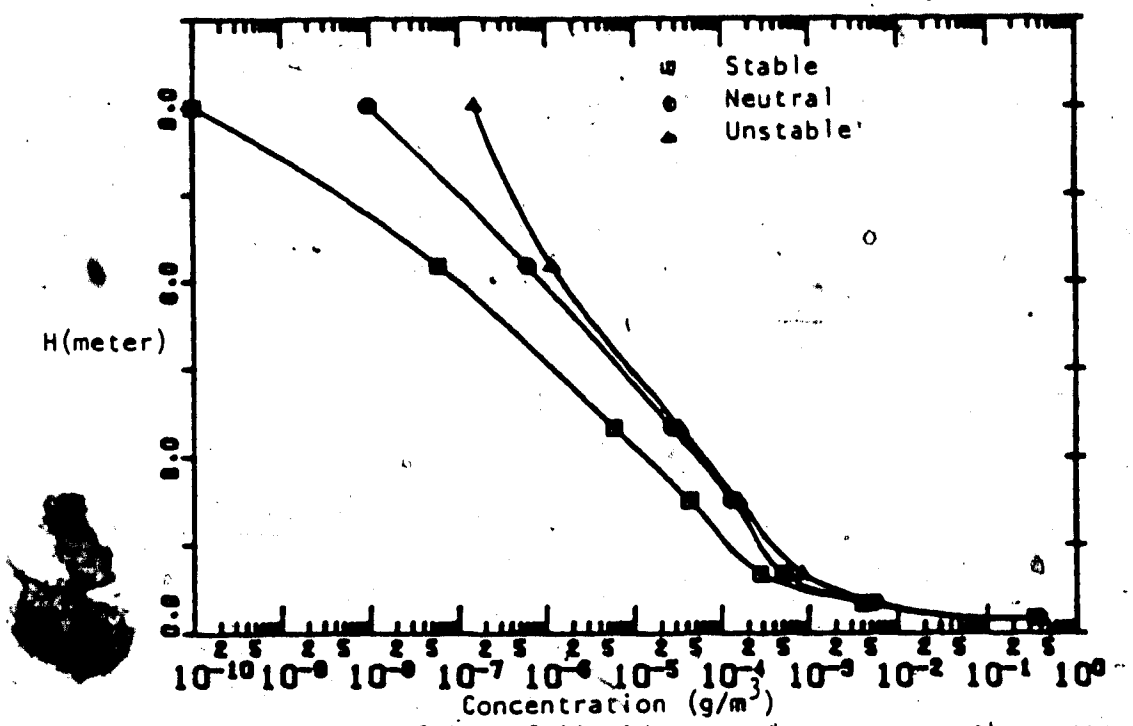

Fig.12 Vertical profiles of liquid water content over the ocean surface

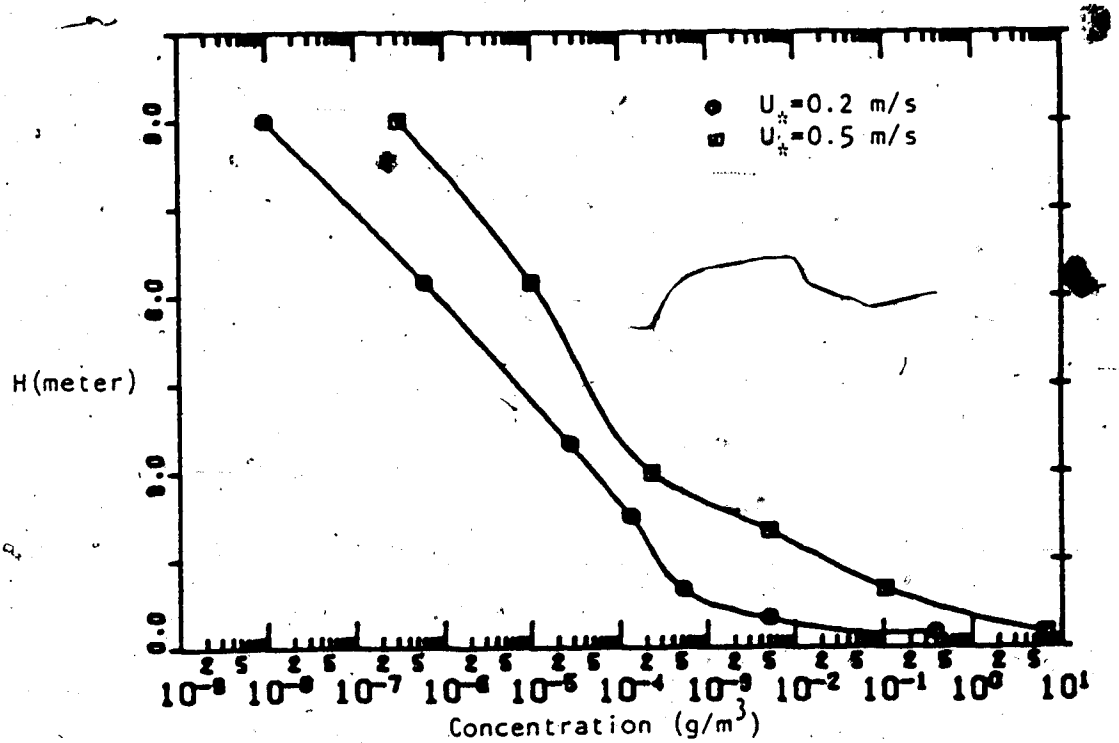

Fig.13 Wind dependence of the profiles of liquid water content

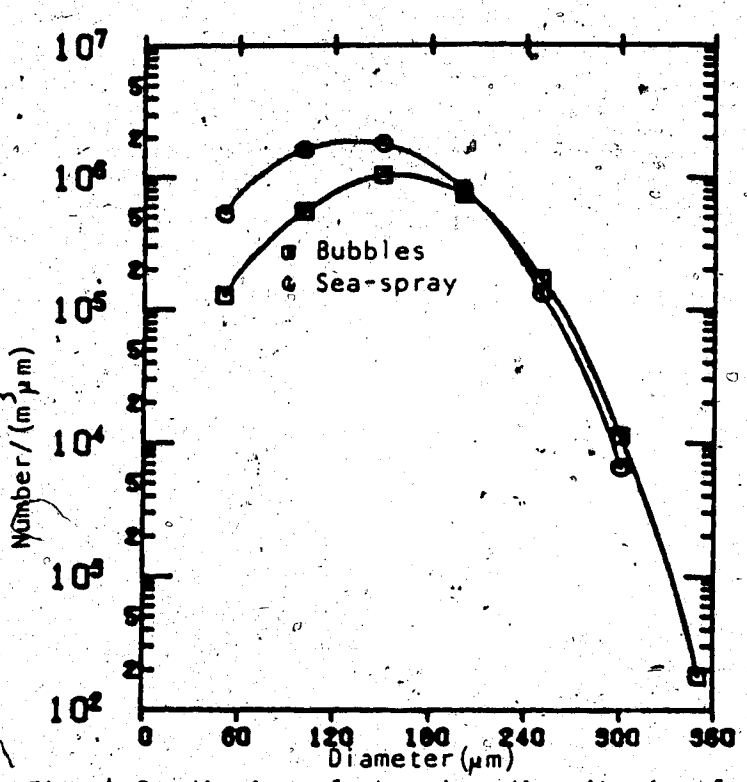

Fig.14 Prediction of the size distribution function of sea-spray at 10cm above the ocean surface

4. Discussion and suggestions for further research

The present study has demonstrated that it is possible to calculate sea-spray concentration profile using a turbulent trajectory simulation approach, provided the initial conditions are well defined.

The main advantage of this approach is that it is in principle equally applicable to both complex and simple situations. There are several questions which should be noted and merit further investigation. Firstly, in formulating the model of heavy particle trajectories we did not consider the correlation between velocity fluctuations, w',u'. Further particle trajectory models should take this into account. Secondly, the major sources of uncertainty in this simulation are the droplet emission characteristics such as the droplet initial size distributions, emission rates and the speeds of the spray droplets. Measurements of spray ejection rates and speeds as a function of size are necessary. Finally, the large spray drops produced by wave collisions with ships, islands etc, have not been included in this study because of the complexity of the generating mechanism. However, by making some simplifications, it might be possible to predict the particle distribution on a ship deck or an island by following their trajectories (in this case one has the added complexity of a disturbed underlying airflow). It should also be noted that the turbulent trajectory model is applicable to some other particle motions in the atmosphere, provided the density of the particle is much higher than that of the air. An example might include the motion of heavy-particle pollutants in the atmosphere.

Bibliography

Angelidou, C. et al(1979): Size distribution functions of dispersions, Chem. Eng. Sci., 34, P.671-676.

Beard, K.V. &H.R. Pruppacher(1971): A wind tunnel investigation of rate of evaporation of small water drops falling at terminal velocity in the air, J. Atmos. Sci., 28, P.1455-1464.

Blanchard, D.C.(1963): Electrification of the Atmosphere by particles from bubbles in the sea, Prog. Oceanogr. 1., P.71-202.

Blanchard, D.C.,&A.H. Woodcock(1957): Bubble formation and modification in the sea and its meteorological significance, Tellus, 9, P.145-158.

Caughey, S.J., Wyngaard, J.C. and Kaimal, J.C.(1979): Turbulence in evolving stable boundary layer, ibid., 36, P.1041-1052

Csanady, G.T.(1963): Turbulent diffusion of heavy particles in the atmosphere, J. Atmos. Sci., 20, P.201-298.

Dyer, A.J.(1974): A review of flux-profile relationships, Ibid., 7, P.363-372.

Faeth, G.M.(1986): Turbulence/Drop interactions in sprays. AIAA paper, No. 86-0136.

Hinze, J.O.(1975): Turbulence, 2nd Ed., McGraw-Hill, New York.

Hunt, J.C.&P. Nalpanis(1985): Saltating and suspended particles over flat and sloping surfaces. 1. Modelling concepts, Proceedings of the international workshop on physics of blown sand, Arhuis. Denmark, Vol.1.

Kerman, B.R.(1986): Distribution of bubbles near the ocean surface, Atmosphere-ocean, 24, P.169-188.;

——— On aerosol production and enrichment by breaking wind waves, Atmosphere-ocean, 24, P.329-345.

Kolovayer, D.A.(1976): Investigation of the concentration and statistical size distribution of wind-produced bubbles in the near-surface layer, Oceanology 15, P.659.

Ley, A.J. and D.J. Thomson(1983): A random walk model of dispersion in the diabatic surface layer, Quart. J. R. Met. Soc., 109, P.867-880.

Lumley, J.L.(1957): Some problems connected with the motion of small particles in turbulent fluid, Ph.D thesis, Johns Hopkins Univ. Baltimore.

Mason, B.J.(1954): Bursting of bubbles at the surface of sea water, Nature, 174, P.470-471.

Meek, C.C.&B.G. Jones(1973): Studies of the behaviour of heavy particles in turbulent fluid flow, J. Atmos. Sci., 30, P.239-244.

Monin, A.S. and A.M. Obukhov(1954): Basic laws of turbulent mixing in the atmosphere near the ground, Tr. Akad. Nauk SSSR Geofiz. Inst., No. 24(151), P.165-187.

Moore, D.W.(1959): The rise of a gas bubble in a viscous liquid, J. Fluid Mech., 6, P.113.

Newitt, D.M., Dombrowski, N., and Kndman, F.H (1954): Liquid entrainment.1, The mechnism of drop formation from gas or

vapor bubbles, Trans. Inst. Chem. Engrs. 32, P.244-261.

Panofsky, H.A., Tennekes, H., Lenschow, D.H. and Wyngaard, J.C.(1977): The characterics of turbulent velocity components in surface layer under convective conditions. ibid., 11, P. 355-362.

Peskin, R.L.(1962): The diffusivity of small suspended particles in turbulent fluids, National meeting A. J. Ch. E., Baltimore.

Reid, J.D.(1979): Markov chain simulations of vertical dispersion in the neutral surface layer for surface and elevated release, Boundary-Layer Meteorology, 16, 3-22.

Schlichting, H.(1960): Boundary Layer theory, McGraw-Hill, New York

Schmitt, K.F. et al (1979): Structure of marine surface layer turbulence, J. Atmos. Sci., 36, P.602-618.

Snyder, W.H.&J.L.Lumley(1971): Some measurements of particle velocity autocorrelation functions in a turbulent flow, J. Fluid Mech., 48, P.41-71.

Soo, S.L.(1967): Fluid Dynamics of multiphase system, Blaisdel Publishing Co., Toronto

Takeda, A.(1981): Effects of wave motions on spectral characteristics of wind fluctuations in the marine atmospheric surface layer. J. of Meteor. Soc. Japan, 59, P.487-508.

Walklate, P.J.(1987): A random-walk model for dispersion of heavy particles in turbulent flow, Boundary-Layer Meteorology,39, P.175-190

Wilson, J.D. et al(1981): Calculation of particle trajectories in the presence of a gradient in turbulent-velocity variance.

Boundary-Layer Meteorology, 27, P.163-169.

Wilson, J.D. et al (1987): Comments on a relationship between fluid and immersed-particle velocity fluctuations proposed by Walklate (1987).

Wu, J.(1981): Evidence of sea spray produced by bursting bubbles, Science, 212, P.324-326.

Wu, J. et al(1984): Production and distributions of sea spray, J. Geophys. Res. 89. P.8163-8169.

Yudine, M.I.(1959): Physical considerations on heavy-particle diffusion, Advances in Geophysics, Vol.6. P.185-191.

Appendix A

A computer program of calculating the number distribution of sea spray at10cm above the ocean surface.

```
 10 OPEN "SPRAYN" FOR OUTPUT AS #1
 20 DIM T(11),Q(50),CONCEN(50)
 30 REM NUMBER DISTRIBUTION OF SEA SPRAY AT 10CM
 40 REM NEUTRAL CASE
 50 Z00=.002:USTAR=.2:MOL=100:DBAR=.00015
 60 NT=200:NP=7:XMAX=100:CONST=.1:GAMMA=.073
 70 V=.0000151:DENSA=1.18:G=9.8:TWOPIE=2*3.1416
 80 DIFK=.000022:RV=[illegible]:P=1000:SC=V/DIFK:DENSP=1000
 90 TLO=.26*Z00/USTA[illegible]T=.1*TLO:KV=.4
100 SIGMAU=2.3*USTAR:SIGMAW=1.5*USTAR
110 H=.4*(MOL*USTAR*10000)^.5
120 REM NSTAR IS A FUNCTION OF U*
130 USTARC=.23:USTARB=USTAR/USTARC:RM=1.7543/1000
140 NSTAR=CONST*(USTARB/RM)^3
150 PRINT #1,"Z0,U*,MOL,N*o,DBAR"
160 PRINT #1,Z00,USTAR,MOL,NSTAR,DBAR
170 PRINT #1,"NP,NT,XMAX,CONST"
180 PRINT #1,NP,NT,XMAX;CONST
190 PRINT #1,"RELATIVE HUMIDITY,TEMPERATURE"
200 PRINT #1,RH,TEMP

210 PRINT #1,"diameter      Concentration"
220 RANDOMIZE TIMER
230 FOR I=1 TO NP
240 REM D IS SPRAY DIAMETER
250 D=.00005+(I-1)*.00005:DD=.00002/DBAR
260 DONDBAR=D/DBAR:DD=.00002/DBAR:VD=1238115!**D^2!
270 REM NUMBER IS THE NUMBER DISTRIBUTION FUNCTION
280 NUMBER=INT(3*NSTAR*(DONDBAR^2)*EXP(-DONDBAR^3)*DD)
290 Q(I)=NUMBER*VD
300 WO=.0000067*(100*P+.6*GAMMA/D)/(DENSP*D)
310 PRINT "PARTICLE #"; I
320 FOR J=1 TO NT
330 DT=.1*TLO
340 UBAR=0!
350 X=0:Z=Z00:WP=WO:UP=0
360 RINED=0
370 GOSUB 790:QW=R:QWO=QW:WA=QW*SIGMAW:WAO=WA:ZO=Z
380 GOSUB 790:QU=R:QUO=QU:UAA=QU*SIGMAU:UAO=UAA:XO=X
390 UA=UBAR+UAA:XA=X:ZA=Z
400 ZPREV=Z:XPREV=X
```

```
410 Z=Z+WP*DT:X=X+UP*DT
420 ZA=ZA+WA*DT:XA=XA+UA*DT
430 Z0=Z0+WA0*DT:X0=X0+(UA0+UBAR)*DT
440 DW=WA-WP:DU=UA-UP
450 RELVEL=SQR(DW*DW+DU*DU)
460 RE=D*RELVEL/V:CDXREL=24*V*(1+(RE^.667)/6)/D
470 A=.75*CDXREL*DENSA/(DENSP*D)
480 WP=(WA-G/A)*(1-EXP(-A*DT))+WP*EXP(-A*DT)
490 UP=UA+(UP-UA)*EXP(-A*DT)
500 IF Z <= Z00 GOTO 710
510 IF Z > 10! GOTO 710
520 IF Z < .2 THEN 530 ELSE 550
530 DDZ=Z-ZPREV:DDX=X-XPREV
540 T(I)=T(I)+SQR((DDZ*DDZ+DDX*DDX)/(WP*WP+UP*UP))
550 IF X >=XMAX GOTO 710
560 UBAR=(USTAR/KV)*(LOG(Z/Z00))
570 TL=.26*Z/USTAR:DT=.1*TL
580 LFG=SIGMAW*TL
590 DZ=ABS(ZA-Z):DX=ABS(XA-X)
600 ALPHA1=EXP(-DT/TL)

605 BETA1=SQR(1.0-ALPHA1*ALPHA1)
610 ALPHAW=EXP(-DT/TL-(DX+DZ)/LFG)
620 BETAW=SQR(1!-ALPHAW*ALPHAW)
630 ALPHAU=ALPHAW:BETAU=SQR(1!-ALPHAU*ALPHAU)
640 GOSUB 790:QW0=ALPHA1*QW0+BETA1*R:WA0=QW0*SIGMAW
650 GOSUB 790:QW=ALPHAW*QW+BETAW*R:WA=QW*SIGMAW
660 GOSUB 790:QU0=ALPHA1*QU0+BETA1*R:UA0=QU0*SIGMAU
670 GOSUB 790:QU=ALPHAU*QU+BETAU*R:UAA=QU*SIGMAU
680 RINED=SQR((X-X0)*(X-X0)+(Z-Z0)*(Z-Z0))
690 IF RINED >= 1.33333*LFG GOTO 360
700 GOTO 390
710 NEXT J
720 NEXT I
730 FOR I=1 TO NP
740 T(I)=T(I)/NT
750 CONCEN(I)=T(I)*Q(I)/.2
760 PRINT #1,50+(I-1)*20,Q(I),CONCEN(I)
770 NEXT I
780 END
790 IF RND <= 0 GOTO 810

800 R=SQR(-2*LOG(RND))*COS(TWOPIE*RND)
810 RETURN
```

Appendix B

A computer program for numerical simulation of Snyder and Lumley's experiment.

```
 10 OPEN "TESTDA" FOR OUTPUT AS #1
 20 DIM XBARSQ(50),YBARSQ(50),XAVG(50),YAVG(50),BASQ(50),AVG(50)
 30 PRINT #1,"heavy.particle diff test,DENSP=8900":KK=2:GOTO 60
 40 PRINT #1,"DENSP=1000":KK=4:GOTO 60
 50 PRINT #1,"DENSP=260":KK=10
 60 WBAR=6.55:V=.0000151:DENSA=1.18:G=9.8:TWOPIE=2*3.1416
 70 D=.0000465:DENSP=8900:TP=.049:DT=.1*TP
 80 IF KK=4 THEN D=.000087:DENSP=1000:TP=.02:DT=.2*TP
 90 IF KK=10 THEN D=.0000465:DENSP=260:TP=.0017:DT=TP
100 NP=1000
110 RANDOMIZE TIMER
120 PRINT #1,"   D            DENSP            NP"
130 PRINT #1,D,DENSP,NP
140 FOR IP=1 TO NP
150 PRINT "PARTICLE #"; IP
160 DRUU=0:DRWW=0:DRWU=0:DX=0:DY=0:DZ=0
170 TL=.45*.0034*((32)^.5)/.3689
175 IF DT > .1*TL THEN DT=.1*TL
180 M=1:MTP=.05

210 RINED=0
220 IF Z < 0 THEN Z=0
230 REM SET THE ORIGINAL FLUID ELEMENT
240 GOSUB 1190
250 GOSUB 1150:QW=R:WAP=QW*SIGMAW:QWO=QW:WAPO=WAP:ZO=Z
260 GOSUB 1150:QU=R:UA=QU*SIGMAU:QUO=QU:UAO=UA:XO=X
270 GOSUB 1150:QV=R:VA=QV*SIGMAV:QVO=QV:VAO=VA:YO=Y
280 WA=WBAR+WAP:XA=X:YA=Y:ZA=Z
290 Z=Z+WP*DT:X=X+UP*DT:Y=Y+VP*DT
300 XA=XA+UA*DT:YA=YA+VA*DT:ZA=ZA+WA*DT
310 ZO=ZO+(WBAR+WAPO)*DT:XO=XO+UAO*DT:YO=YO+VAO*DT
320 DW=WA-WP:DU=UA-UP:DV=VA-VP
330 RELVEL=SQR(DU*DU+DV*DV+DW*DW)
340 RE=D*RELVEL/V:CDXREL=24*V*(1+(RE^.667)/6)/D
350 A=.75*CDXREL*DENSA/(DENSP*D):NA=NA+A:SS=SS+1
360 WP=(WA-G/A)*(1-EXP(-A*DT))+WP*EXP(-A*DT)
370 UP=UA+(UP-UA)*EXP(-A*DT)
380 VP=VA+(VP-VA)*EXP(-A*DT)
390 DZ=ABS(Z-ZA):DX=ABS(X-XA):DY=ABS(Y-YA)
400 DRUU=SQR(DX*DX+DY*DY):DRWW=SQR(DZ*DZ+DY*DY)
```

```
410 DRWU=SQR(DZ*DZ+DX*DX)
420 IF Z < 0 THEN Z=0
430 GOSUB 1190
440 LF=.0034*((100*Z/2.54+32)^.5):LG=.45*LF:TL=LG/SIGMAU
445 IF DT > .1*TL THEN DT=.1*TL
450 ALPHA1=EXP(-DT/TL):BETA1=SQR(1!-ALPHA1*ALPHA1)
460 ALPHAW=EXP(-DT/TL-DRUV/LG-DZ/LF):BETAW=SQR(1!-ALPHAW*ALPHAW)
470 ALPHAU=EXP(-DT/TL-DRWV/LG-DX/LF):BETAU=SQR(1!-ALPHAU*ALPHAU)
480 ALPHAV=EXP(-DT/TL-DRWU/LG-DY/LF):BETAV=SQR(1!-ALPHAV*ALPHAV)
490 GOSUB 1150:QWO=ALPHA1*QWO+BETA1*R:WAPO=QWO*SIGMAW
500 GOSUB 1150:QW=ALPHAW*QW+BETAW*R:WAP=QW*SIGMAW
510 GOSUB 1150:QUO=ALPHA1*QUO+BETA1*R:UAO=QUO*SIGMAU
520 GOSUB 1150:QU=ALPHAU*QU+BETAU*R:UA=QU*SIGMAU
530 GOSUB 1150:QVO=ALPHA1*QVO+BETA1*R:VAO=QVO*SIGMAV
540 GOSUB 1150:QV=ALPHAV*QV+BETAV*R:VA=QV*SIGMAV
550 IF Z >= 1.229 GOTO 590
560 RINED=SQR((X-XO)*(X-XO)+(Y-YO)*(Y-YO)+(Z-ZO)*(Z-ZO))
570 IF RINED >= LG GOTO 210
580 GOTO 280
590 X1=X:Y1=Y:Z1=Z:T=0
600 RINED=0

610 IF Z < 0 THEN Z=0
620 GOSUB 1190
630 GOSUB 1150:QW=R:WAP=QW*SIGMAW:QWO+QW:WAPO=WAP:ZO=Z
640 GOSUB 1150:QU=R:UA=QU*SIGMAU:QUO=QU:UAO=UA:XO=X
650 GOSUB 1150:QV=R:VA=QV*SIGMAV:QVO=QV:VAO=VA:YO=Y
660 WA=WBAR+WAP:XA=X:YA=Y:ZA=Z
670 ZO=ZO+(WBAR+WAPO)*DT:XO=XO+UAO*DT:YO=YO+VAO*DT
680 Z=Z+WP*DT:X=X+UP*DT:Y=Y+VP*DT
690 ZA=ZA+WA*DT:XA=XA+UA*DT:YA=YA+VA*DT
700 DW=WA-WP:DU=UA-UP:DV=VA-VP
710 RELVEL=SQR(DU*DU+DV*DV+DW*DW)
720 RE=D*RELVEL/V:CDXREL=24*V*(1+(RE^.667)/6)/D
730 A=.75*CDXREL*DENSA/(DENSP*D):NA=NA+A:SS=SS+1
740 WP=(WA-G/A)*(1-EXP(-A*DT))+WP*EXP(-A*DT)
750 UP=UA+(UP-UA)*EXP(-A*DT)
760 VP=VA+(VP-VA)*EXP(-A*DT)
770 DZ=ABS(Z-ZA):DX=ABS(X-XA):DY=ABS(Y-YA)
780 DRUV=SQR(DX*DX+DY*DY):DRWU=SQR(DZ*DZ+DY*DY)
790 DRWU=SQR(DZ*DZ+DX*DX)
800 IF Z < 0 THEN Z=0
810 GOSUB 1190
820 LF=.0034*((100*Z/2.54+32)^.5):LG=.45*LF:TL=LG/SIGMAU
```

```
820 LF=.0034*((100*Z/2.54+32)^.5):LG=.45*LF:TL=LG/SIGMAU
830 ALPHA1=EXP(-DT/TL):BETA1=SQR(1!-ALPHA1*ALPHA1)
840 ALPHAW=EXP(-DT/TL-DRUV/LG-DZ/LF):BETAW=SQR(1!-ALPHAW*ALPHAW)
850 ALPHAU=EXP(-DT/TL-DRWV/LG-DX/LF):BETAU=SQR(1!-ALPHAU*ALPHAU)
860 ALPHAV=EXP(-DT/TL-DRWU/LG-DY/LF):BETAV=SQR(1!-ALPHAV*ALPHAV)
870 GOSUB 1150:QW0=ALPHA1*QW0+BETA1*R:WAP0=QW0*SIGMAW
880 GOSUB 1150:QW=ALPHAW*QW+BETAW*R:WAP=QW*SIGMAW
890 GOSUB 1150:QU0=ALPHA1*QU0+BETA1*R:UA0=QU0*SIGMAU
900 GOSUB 1150:QU=ALPHAU*QU+BETAU*R:UA=QU*SIGMAU
910 GOSUB 1150:QV0=ALPHA1*QV0+BETA1*R:VA0=QV0*SIGMAU
920 GOSUB 1150:QV=ALPHAV*QV+BETAV*R:VA=QV*SIGMAV
930 T=T+DT
940 IF T >= MTP GOTO 980
950 RINED=SQR((X-X0)*(X-X0)+(Y-Y0)*(Y-Y0)+(Z-Z0)*(Z-Z0))
960 IF RINED >= LG GOTO 600
970 GOTO 660
980 XBARSQ(M)=XBARSQ(M)+(X-X1)*(X-X1):XAVG(M)=XAVG(M)+X
990 YBARSQ(M)=YBARSQ(M)+(Y-Y1)*(Y-Y1):YAVG(M)=XAVG(M)+Y
1000 MTP=MTP+.05:M=M+1
1010 IF M >=10 GOTO 1030
1020 GOTO 660
1030 NEXT IP
1030 NEXT IP
1040 FOR N=1 TO 9
1050 BASQ(N)=(XBARSQ(N)+YBARSQ(N))/(2*NP)
1051 AVG(N)=(XAVG(N)+YAVG(N))/(2*NP)
1060 PRINT #1,N,BASQ(N),AVG(N)
1070 BASQ(N)=0:XBARSQ(N)=0:YBARSQ(N)=0
1080 NEXT N
1075 AVG(N)=0:XAVG(N)=0:YAVG=0
1090 PRINT #1,"RAVG/NR                                    RSQR/NR"
1100 PRINT #1,RAVG/NR,RSQR/NR
1110 PRINT #1,"NA/SS=",NA/SS
1120 RAVG=0:NR=0:RSQR=0:NA=0:SS=0
1130 IF KK=2 GOTO 40
1140 IF KK=4 THEN 50 ELSE END
1150 IF RND < = 0 GOTO 1180
1160 R=SQR(-2*LOG(RND))*COS(TWOPIE*RND)
1170 RAVG=RAVG+R:RSQR=RSQR+R*R:NR=NR+1
1180 RETURN
1190 SIGMAW=6.55/SQR(42.4*(100*Z/2.54+4))
1200 SIGMAU=6.55/SQR(39.4*(100*Z/2.54+8))
1210 SIGMAV=SIGMAU
1220 RETURN
```